

## Supplementary Information

### Biphenylene Network as Sodium Ion Battery Anode Material

Xin-Wei Chen, Zheng-Zhe Lin\*, Xi-Mei Li

*School of Physics, Xidian University, Xi'an 710071, China*

\* Corresponding Author. E-mail address: [zzlin@xidian.edu.cn](mailto:zzlin@xidian.edu.cn)

#### 1. Hybrid Functional Calculation on BPN-Na Systems

In this section, the calculation results of the PBE functional is compared with the results of hybrid HSE06 functional. We first check the energy bands. **Fig. S1** shows the energy bands of BPN monolayer at the level of PBE and HSE06. Since BPN is a metal, the PBE functional is able to describe the energy bands. Within the PBE and HSE06 functionals, the described energy bands near the Fermi level are similar.

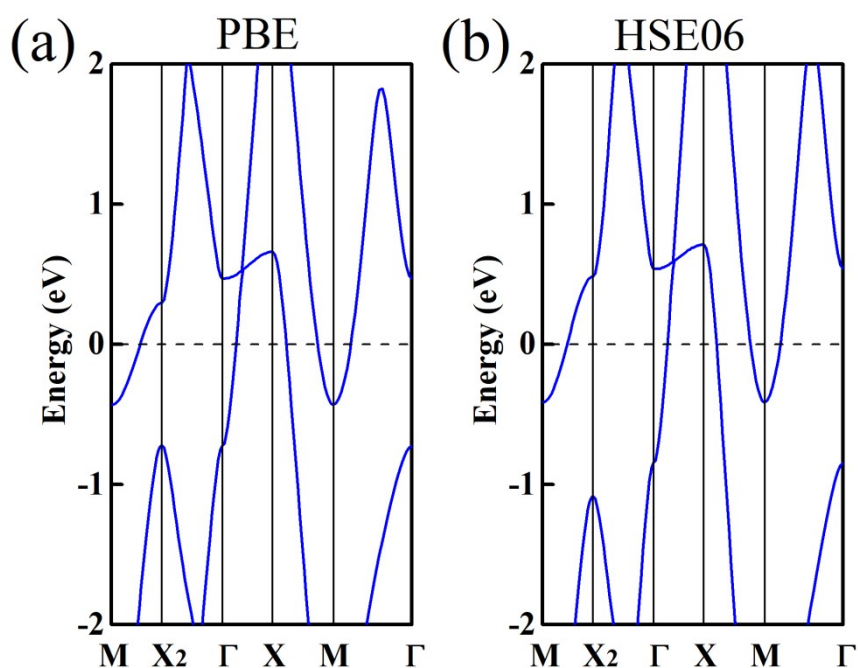


**Fig. S1** The energy bands of BPN monolayer at the level of (a) PBE and (b) HSE06.

Then, we verify the PBE calculations results of BPN-Na systems with the HSE06 functional. The main conclusion is focused on the formation energies of  $\text{Na}_x\text{C}_6$  systems

and the OCV (decided by the convex hull of  $\text{Na}_x\text{C}_6$ ). Since the HSE06 functional leads to large computation cost, we first obtain the convex hull by calculating the formation energies of more than one hundred  $\text{Na}_x\text{C}_6$  systems at the level of PBE, and then calculate the formation energies of the  $\text{Na}_x\text{C}_6$  configurations on the convex hull at the level of HSE06. **Fig. S2(a)** shows the comparison of the  $\text{Na}_x\text{C}_6$  convex hull at the level of the two functionals. Then, the OCV profile is calculated by Eq. (4) (**Fig. S2(b)**). The two functionals exhibit a same trend on the formation energies in the convex hull and the OCV profile. Within the PBE functional, the lowest formation energy in the convex hull is  $E_f = -0.67$  eV, and the OCV in the main charging section of BPN-Na anode ( $x = 0 \sim 0.889$ ) is +0.68 V. Within the HSE06 functional, the lowest formation energy in the convex hull is  $E_f = -0.77$  eV, and the OCV in the main charging section of BPN-Na anode ( $x = 0 \sim 0.889$ ) is +0.73 V.

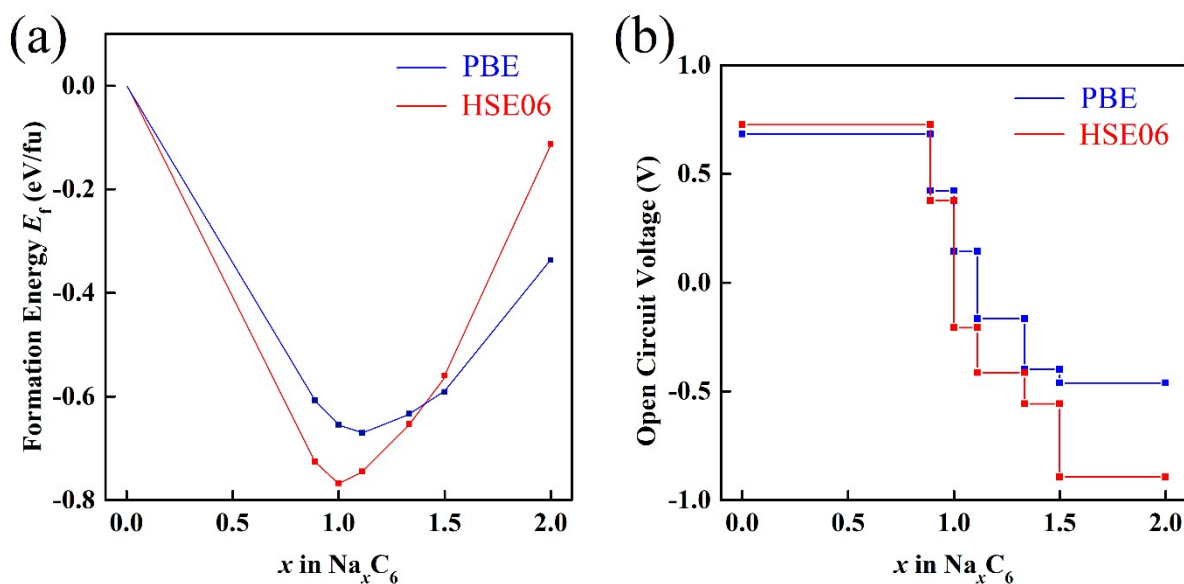


**Fig. S2 (a)** The formation energies  $E_f$  of the structures on the convex hull at the level of PBE and HSE06. **(b)** OCV profiles as the function of Na concentration  $x$  at the level of PBE and HSE06.

## 2. Na adsorption on BPN Monolayer

Here we compare the formation energy of Na on free-standing BPN monolayer with Na on BPN bulk. Na atoms prefer locating at the octagonal C rings of BPN. In the

Na full state, i.e. NaC<sub>6</sub>, every octagonal C ring is occupied by one Na atom. According to Eq. (3), the formation energy of NaC<sub>6</sub> is

$$E_f = E_{uc}(\text{BPN-Na}) - E_{uc}(\text{BPN}) - E(\text{Na})$$

For BPN monolayer, the formation energy of NaC<sub>6</sub> ( $E_f = +0.14$  eV), which is larger than zero, is disadvantageous to Na adsorption. This result is coincident with the reference *Phys. Chem. Chem. Phys.* **24**, 10712 (2022), which reported that the average Na adsorption on BPN monolayer increase with enlarging  $x$ . By contrast, the formation energy of NaC<sub>6</sub> in BPN bulk is  $E_f = -0.65$  eV, which is much lower than that in BPN monolayer.

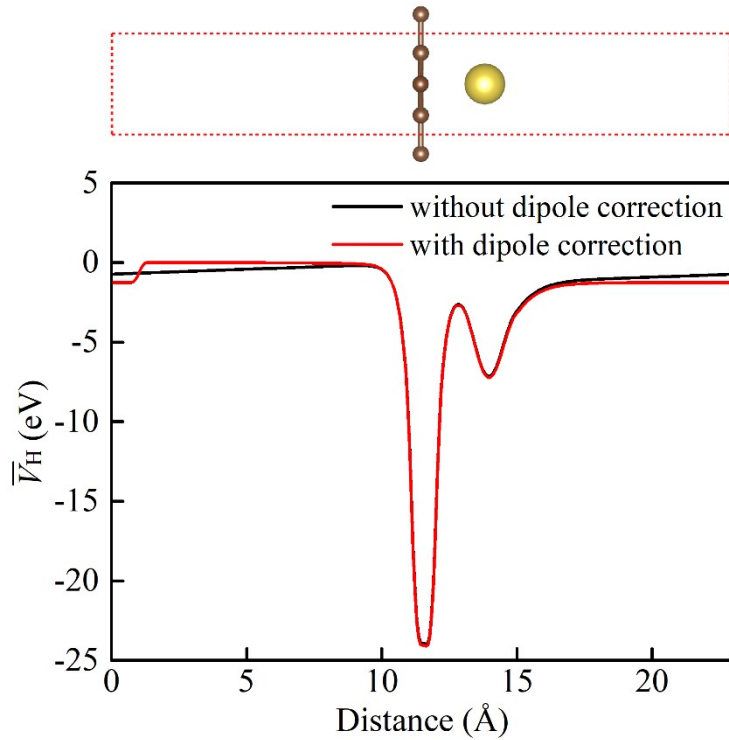


**Fig. S3** Average Hartree potential  $\bar{V}_H$  of BPN-Na monolayer with / without dipole correction.

In asymmetric two-dimensional systems, the charge transfer can result in a net dipole moment that affects the calculation results. To account for this, dipole correction is always employed in *ab initio* calculations. To verify the effect of dipole correction on our results, the average Hartree potential

$$\bar{V}_H(z) = \frac{1}{S} \int V_H(\mathbf{r}) dx dy$$

is defined along the  $z$  direction perpendicular to the two-dimensional system. Here,  $V_H(\mathbf{r})$  is the Hartree potential at position  $\mathbf{r}$ . The equation takes the average in the  $xy$  plane. **Fig. S3** shows  $\bar{V}_H(z)$  in the monolayer  $\text{NaC}_6$  system with and without dipole correction. We can see that the distinction is small. In addition, with dipole correction, the calculated the formation energy of monolayer  $\text{NaC}_6$  is only 0.003eV higher than that without dipole correction. So, it can be concluded that the influence of dipole can be ignored.

### 3. MD Simulation and Lattice Stability

To verify the thermal stability of bulk BPN, we perform *ab initio* MD simulations for AA and AB stacking patterns at 300 K. The simulation supercell is taken as  $3 \times 3 \times 4$ . The time step is set to 1 fs. After a pre-equilibrium of 1 ps, the simulations last 4 ps. **Fig. S4 (a)** and **(b)** show the potential energy profiles of AA and AB supercells in the simulations, respectively. In **Sec. 3.1**, we show that the binding energies are close. In the molecular dynamics simulations, we can see that their average potential energies and potential energy fluctuations are similar. The final evolution of AA and AB supercells can be seen in the subfigures of **Fig. S4 (a)** and **(b)**.

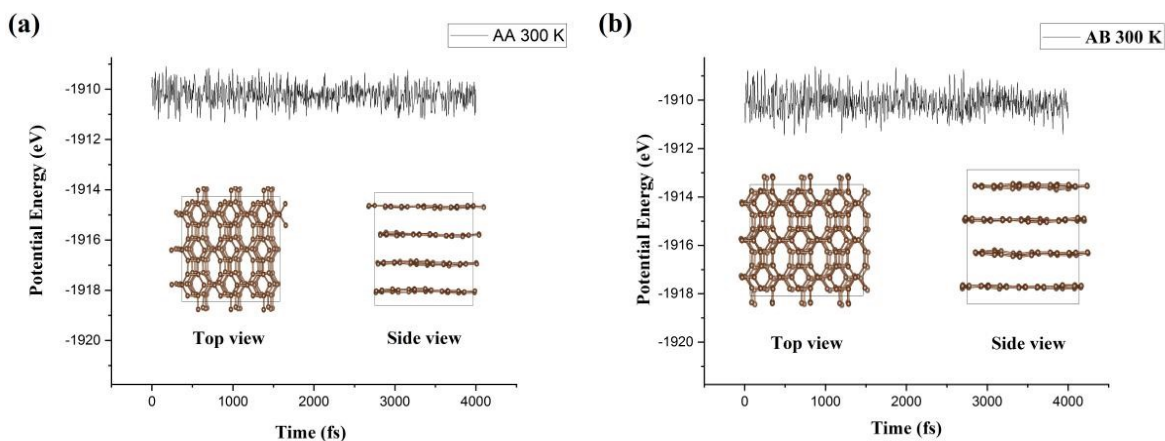


**Fig. S4** The evolution of the potential energy of  $3 \times 3 \times 4$  bulk BPN with **(a)** AA and **(b)** AB stacking patterns at 300 K. The final structures are shown in the subfigures.

MD simulations are also performed for  $\text{Na}_x\text{C}_6$ . We choose  $\text{Na}_{1.111}\text{C}_6$  that has the

lowest formation energy, and  $\text{Na}_2\text{C}_6$  that has maximum Na concentration. **Fig. S5 (a)** and **(b)** correspondingly show their potential energy profiles. The final configurations can be seen in the subfigures.

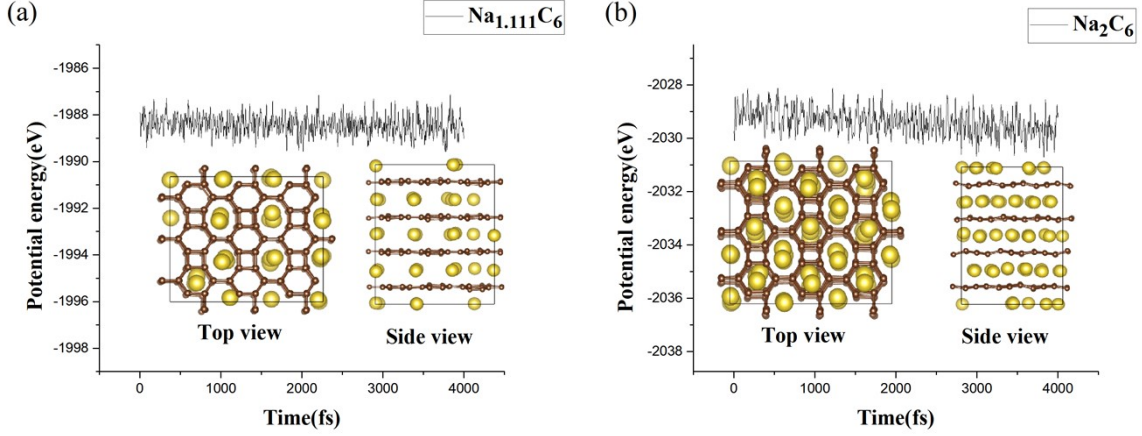


**Fig. S5** The evolution of the potential energy of  $3\times 3\times 4$  bulk BPN-Na phase at 300 K. **(a)**  $\text{Na}_{1.111}\text{C}_6$ . **(b)**  $\text{Na}_2\text{C}_6$ . The final structures are shown in the subfigures.

#### 4. COHP of Graphite

To understand the C-C bonding, projected COHP [*J. Phys. Chem. A* **115**, 5461 (2011)] are calculated. For atomic orbitals  $|\mu\rangle$  and  $|\nu\rangle$ , the projected COHP is defined as

$$\text{COHP}_{\mu\nu}(E) = \sum_{\mathbf{k}j} \langle \mu | \psi_j(\mathbf{k}) \rangle \langle \psi_j(\mathbf{k}) | \nu \rangle \langle \nu | \mathbf{H} | \mu \rangle \delta(E - \varepsilon_j(\mathbf{k})),$$

where  $\mathbf{H}$  is the PAW Hamiltonian,  $|\psi_j(\mathbf{k})\rangle$  is the  $j$ -th Bloch state at the  $\mathbf{k}$  point and  $\varepsilon_j(\mathbf{k})$  is the energy of  $|\psi_j(\mathbf{k})\rangle$ . Negative COHP describes bonding combination. Positive COHP describes anti-bonding combination. Here, the COHP is calculated by taking the average of COHP between atomic orbitals of nearest C-C atoms. The COHP values below the Fermi level are negative (i.e. bonding), while above the Fermi level are positive (i.e. anti-bonding). This feature indicates perfect C-C bonding.

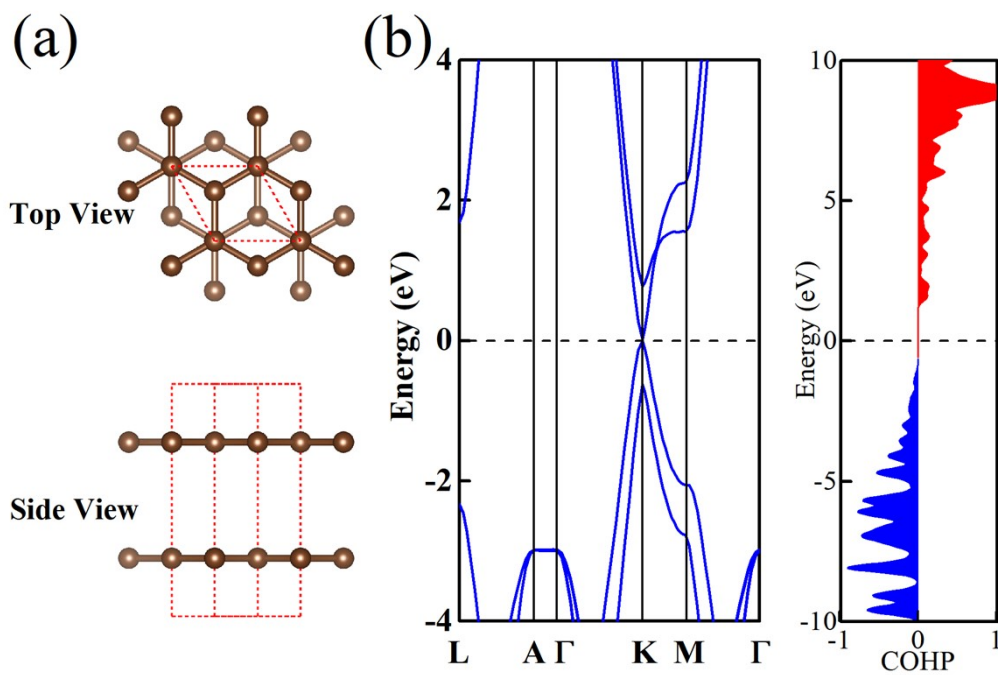


**Fig. S6** (a) The structure of graphite. (b) The energy bands and COHP of graphite. The COHP is calculated by averaging the atomic orbitals of nearest C-C pairs.